

## Analysis of Er<sup>3+</sup> Incorporation in SnO<sub>2</sub> by Optical Investigation

Evandro A. de Moraes\*, Luis V. A. Scalvi\*, Márcio R. Martins\*, and Sidney J. L. Ribeiro†

\*Dep. Física – Faculdade de Ciências – POSMAT, UNESP- Universidade Estadual Paulista, Caixa Postal 473, 17033-360 Bauru – SP, Brazil

†Instituto de Química de Araraquara – UNESP Universidade Estadual Paulista, Caixa Postal 355, 14801-970, Araraquara - SP, Brazil

Received on 4 April, 2005

Er<sup>3+</sup> emission in the wide bandgap matrix SnO<sub>2</sub> is observed either through a direct Er ion excitation process as well as by an indirect process, through energy transfer in samples codoped with Yb<sup>3+</sup> ions. Electron-hole generation in the tin dioxide matrix is also used to promote rare-earth ion excitation. Photoluminescence spectra as function of temperature indicate a slight decrease in the emission intensity with temperature increase, yielding low activation energy, about 3.8meV, since the emission even at room temperature is rather considerable.

Keywords: Er<sup>3+</sup> emission; SnO<sub>2</sub>; Photoluminescence spectra

### I. INTRODUCTION

In the last decade, rare-earth doped materials earn a significant position in the challenge to finding new optoelectronic devices that can contribute for technological innovation. The behavior of rare-earth atom in semiconductor materials is among the most interesting combination of potential communication devices.

In its threefold oxidation state, rare-earth ions exhibit luminescence due to 4f core transition, which is practically independent of host matrix [1]. In the case of Er<sup>3+</sup> for instance, these transitions yield several emission lines from visible to infrared. In particular, the transition about 1540 nm is of great interest, since it coincides with the minimum optical absorption from silica based optical fibers [1].

Many efforts have been done towards the increase of emission about 1540nm, such as codoping with other trivalent rare-earth ions or oxygen, and the use of wide bandgap semiconductors as host [2]. Electronic structure of Er<sup>3+</sup> determines the optical properties of the resulting material. Besides the oxygen codoping favors luminescence even at room temperature, due to suppression of thermal quenching [2,3]. By the other hand, the use of large wide bandgap matrix also reduces thermal quenching [4], resulting in a very intense luminescence, as observed by Masahi et. al. [3] for TiO<sub>2</sub>. SnO<sub>2</sub> is a wide bandgap semiconductor (3.6eV) and shows high reflectivity in the infrared and fair transparency in the visible, above 90% [5,6]. This feature combined with low electrical resistivity, due to n-type conduction originated from oxygen vacancies and adequate doping, leads to a very attractive material for transparent electrodes, among very many other applications [6,7]. Conjunction of optical properties of SnO<sub>2</sub> and emission from Er<sup>3+</sup> ion presents a potential applicability in optoelectronics devices.

Recently, waveguide properties have been observed in SnO<sub>2</sub>:Er thin films [8]. SnO<sub>2</sub> based nanocomposites doped with rare-earth trivalent ions, obtained by sol-gel route have shown efficient luminescence due to energy transfer processes, such as between Eu<sup>3+</sup> and Tb<sup>3+</sup> [9]. Er-doped SnO<sub>2</sub> can also be used in optical amplifiers and electroluminescent devices where electron-hole energy is transferred to Er<sup>3+</sup> ion. Besides, sol-gel route has shown many advantages

in preparing erbium doped waveguides amplifiers (EDWA) [10-11].

### II. EXPERIMENTAL

Colloidal suspensions have been prepared by sol-gel process. The desired amount of ErCl<sub>3</sub>.6H<sub>2</sub>O was added to an aqueous solution of SnCl<sub>4</sub>.5H<sub>2</sub>O (0.2 mol), under magnetic stirring, followed by addition of NH<sub>4</sub>OH until pH reaches 11. Resulting suspension was submitted to dialysis against distilled water by about 10 days in order to eliminate Cl<sup>-</sup> and NH<sub>4</sub><sup>+</sup> ions. This procedure leads to a stable suspension (sol) of SnO<sub>2</sub>:Er. Yb codoping was obtained by adding SnO<sub>2</sub>:Er powder to an aqueous solution of YbCl<sub>3</sub>.6H<sub>2</sub>O. Xerogels were obtained by just drying the sol at room temperature and pressure. For photoluminescence (PL) measurements at low temperature, the xerogel (powder) was treated at 1000°C during 6 hours and compressed down with 5 × 10<sup>3</sup> kgf/cm<sup>2</sup> of load to the shape of a pellet. PL results shown in this paper have been obtained according to two distinct set-ups: for room temperature data, it was used a xenon lamp of 450W, a fluorimeter SPEX F212I and a germanium detector North Coast Scient. Corporation model EO-8171. For low temperature PL, it was used a Ar<sup>+</sup> laser from Spectra Physics model 2017 for sample excitation and a monochromator Jobin Yvon model T64000. Sample cooling was done in a He closed-cycle cryostat from Janis. A germanium detector from Edinburgh Instruments was used for signal measuring and recording.

### III. RESULTS

Figure 1 shows a diagram explaining the excitation mechanism of SnO<sub>2</sub> xerogels doped with 2at% of Er and codoped with the same amount of Yb. Direct excitation of Er<sup>3+</sup> ions can be obtained through many distinct process, for instance by direct irradiation with: (a) 488nm (<sup>4</sup>I<sub>15/2</sub> → <sup>4</sup>F<sub>7/2</sub>) and (b) 526nm (<sup>4</sup>I<sub>15/2</sub> → <sup>2</sup>H<sub>11/2</sub>). Non-radiative transitions may occur between <sup>4</sup>F<sub>7/2</sub> → <sup>4</sup>I<sub>13/2</sub> and <sup>2</sup>H<sub>11/2</sub> → <sup>4</sup>I<sub>13/2</sub> levels, which are labeled by (c) and (d) in Fig. 1. Indirect excitation (process (e)

in Fig. 1) can be done with the  $\text{Yb}^{3+} \ ^2\text{F}_{7/2} \rightarrow \ ^2\text{F}_{5/2}$  transition (980nm), in codoped samples, since this transition has energy coincident with  $\text{Er}^{3+} \ ^4\text{I}_{11/2} \rightarrow \ ^4\text{I}_{15/2}$  transition. Process (f) shows this energy transfer from  $\text{Yb}^{3+}$  transition to  $\text{Er}^{3+}$  ion. Process (g) is the non-radiative decay  $\ ^4\text{I}_{11/2} \rightarrow \ ^4\text{I}_{13/2}$  and (h) is the emission which comes from  $\ ^4\text{I}_{13/2}$  to the ground state  $\ ^4\text{I}_{15/2}$ . In this work, photoluminescence spectra were obtained under distinct excitation energies, according to some transition shown in Fig. 1. Besides, generation of electron-hole pairs from the  $\text{SnO}_2$  matrix was provided with excitation with 328nm. Photoluminescence of excitation (PLE) were carried out from the ultraviolet to near infrared (300-1000 nm), with fixed emission at 1540 nm.

Figure 2 shows PL spectra for tin dioxide xerogel codoped with 2at% of Er and Yb. Three different excitation wavelengths were used: 328nm (a), 526nm (b) and 980nm (c). In the inset, it is seen PLE with fixed emission at 1540nm.

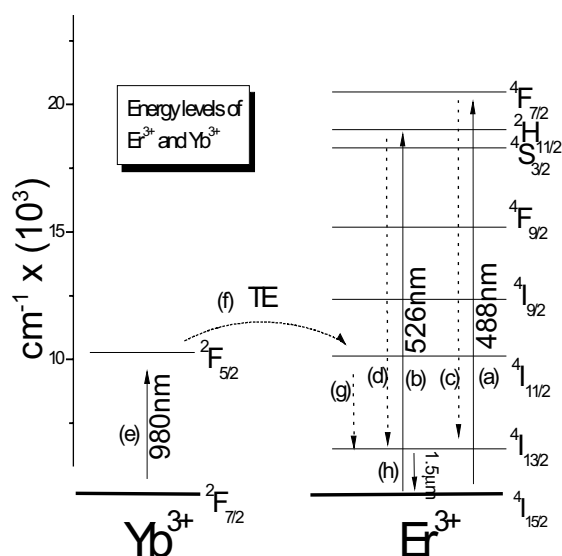


FIG. 1: Energy levels diagram of  $\text{Er}^{3+}$  and  $\text{Yb}^{3+}$ .

A recent investigation of PL spectra [12] of  $\text{SnO}_2:\text{Er},\text{Yb}$  xerogels with doping concentration of 0.1at% yield information on Er localization in the matrix. Two families of Er sites were found in  $\text{SnO}_2$ : substitutional to  $\text{Sn}^{4+}$  and segregated at boundary layer. The second family is related to the solubility limit of rare-earth (RE) ions in tin dioxide, which is about 0.05at%, and the doping excess become located at boundary layer as a  $\text{RE}_2\text{Sn}_2\text{O}_7$  phase [13]. For the high doping concentration (2%) of the samples reported here, it is expected very many Er complexes segregated at boundary layer. Figure 2 shows the emission efficiency of Er at room temperature, excited either directly, curves (a) and (b), or by an energy transfer process from  $\text{Yb}^{3+}$  to  $\text{Er}^{3+}$  ( $\ ^2\text{F}_{5/2} + \ ^4\text{I}_{15/2} \rightarrow \ ^2\text{F}_{7/2} + \ ^4\text{I}_{11/2}$ ), curve (c). When pumping  $\text{Yb}^{3+}$  ions with a monochromatic light of 980 nm of wavelength, Er emission is as observed in Fig. 2(c). In a previous paper [12], it was verified that codoping with  $\text{Yb}^{3+}$  is efficient only for  $\text{Er}^{3+}$  ions located at

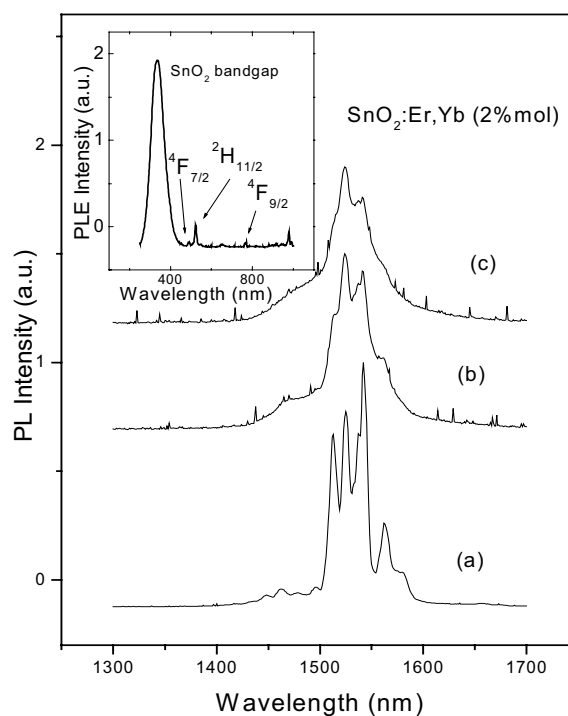


FIG. 2: Photoluminescence (PL) of  $\text{SnO}_2:\text{Er},\text{Yb}$  (2% at.) under excitation at: 328nm (a); 526nm (b) and 980nm (c). Inset: Photoluminescence of excitation (PLE) for the same sample, with fixed emission at 1540nm.

grain boundary. The rare-earth ions located at  $\text{Sn}^{4+}$  sites are not substantially excited by this indirect procedure. The inset in Fig. 2 shows PLE for the same xerogel at room temperature. It is observed a very strong absorption in the bandgap of  $\text{SnO}_2$  matrix due to electron-hole generation, which in turn promotes Er emission seen in Fig. 2(a). It is well known that emission from substitutional sites is easily observed via band-to-band excitation of  $\text{SnO}_2$  [12]. Then, the large band observed by PLE is a strong indication that  $\text{Er}^{3+}$  enters into the lattice, in substitution to Sn atoms. In the inset of Fig. 2 it is also observed intra-ff transitions from ground state  $\ ^4\text{I}_{15/2}$  to excited states  $\ ^4\text{F}_{7/2}$ ,  $\ ^2\text{H}_{11/2}$ ,  $\ ^4\text{S}_{3/2}$  e  $\ ^4\text{F}_{9/2}$ . Some of these states are labeled in the inset of Fig. 2. A peak around 980 nm is also observed, which suggests absorption by  $\text{Yb}^{3+}$  ions.

Figure 3 shows temperature dependence of PL spectra in the range 8 K to 280 K for 2at% Er doped  $\text{SnO}_2$  xerogel. Figure 3(a) shows curves measured at 50 K and 200 K and Fig. 3(b) for 8 K and 280 K. The  $\text{Er}^{3+}$  transition  $\ ^4\text{I}_{13/2} \rightarrow \ ^4\text{I}_{15/2}$  around 1500nm is clearly evidenced by the presence of several peaks. All the recorded spectra were obtained strictly under the same experimental conditions: slit opening in the entrance and the exit of the germanium detector, Ar laser power irradiating the sample (15 mW), and excitation wavelength (488nm), which corresponds to transition of ground state to  $\text{Er}^{3+} \ ^4\text{F}_{7/2}$ .

It can be noticed that temperature decrease leads to PL intensity increase, since the cooling down decreases the lat-

tice vibration of  $\text{SnO}_2$ , and then phonon assisted nonradiative processes, which enhance light emission from  $\text{Er}^{3+}$  core transition. It also can be noticed that details of the low temperature spectra are not observed at higher temperatures. In the measurement carried out at 8 K (Fig. 3(b)), it is clearly seen the presence of a peak about 1555nm, which is not observed at 280 K. This vanishing is probably related to lattice vibration. All the observed peaks are related to the transition of excited state  $^4I_{13/2}$  to the ground state  $^4I_{15/2}$ .

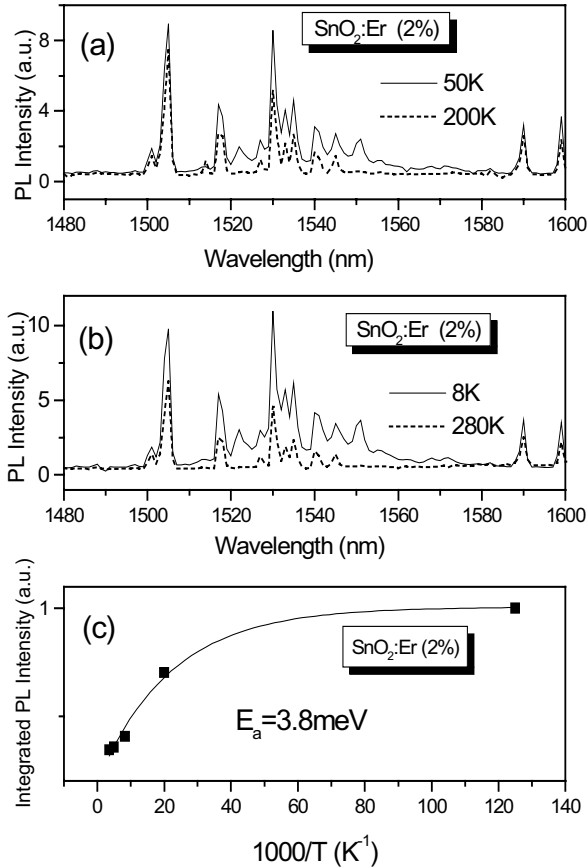


FIG. 3: Temperature dependence of PL for 2at% Er doped  $\text{SnO}_2$  xerogel. (a) Temperatures 50 K and 200K, (b) 8 K and 280K, (c) Integrated intensity of PL as function of reciprocal temperature.

The presence of several peaks can be attributed to the splitting of  $^4I_{13/2}$  and  $^4I_{15/2}$  levels due to the matrix crystalline field. In Si matrix [14] the  $\text{Er}^{3+}$   $^4I_{13/2}$  manifold has its second and third levels located 4.2meV and 8.9 meV from the lowest lying level, respectively. Then a radiative transition from the degenerate  $^4I_{13/2}$  state to the ground  $^4I_{15/2}$  state presents peaks shifted at 9 and 16 nm respectively from the lowest energy level. These upper states of the excited degenerate  $^4I_{13/2}$  level become populated due to local laser heating [14], as evidenced by the fact that such a line splitting does not takes place when the sample is irradiated with monochromatic light coming from a xenon lamp (Fig. 2).

Figure 3(c) shows integrated intensity of PL data for the transition  $^4I_{13/2} \rightarrow ^4I_{15/2}$  as function of  $T^{-1}$ . It is seen that there is a decrease of intensity of luminescence with temperature increase, and a smooth thermal quenching takes place for temperatures above 50 K. The Arrhenius plot yields low activation energy, 3.8meV, compared to Er doped Si single crystal, 150meV [1]. In the latter case the intensity reaches 3 orders of magnitude higher with temperature decrease, being even eliminated at room temperature.

In the case reported in this paper, the magnitude of PL intensity in Er-doped  $\text{SnO}_2$  has varied only one order of magnitude, which explains the low activation energy. This feature may be related to the nonradiative centers which are present at boundary layer due to excess of Er, which reduces the emission efficiency, even at low temperature. It is well-known that in Si matrix, oxygen vacancies increase these nonradiative effects [15]. In our samples this energy may be related to the energy needed to release the electron from the boundary layer defects (potential barrier), to become able of decaying in a radiative or nonradiative way. New measurements with other concentration of Er doping are in progress and shall help the understanding of the temperature dependent process of PL intensity. However it is worthy noting that even at room temperature there is luminescence in Er-doped  $\text{SnO}_2$ , which may become very important for new technological applications.

#### IV. CONCLUSION

Photoluminescence properties of Er-doped tin dioxide in the form of xerogels have been investigated.

Temperature dependent excitation of 2at%Er in  $\text{SnO}_2$  with 488nm promoted the excitation of ions  $\text{Er}^{3+}$  to its  $^4F_{7/2}$  level and the probable decay to nonradiative level  $^4I_{13/2}$ , with subsequent emission to the ground state  $^4I_{15/2}$ , which means emission about de 1540nm. Slight increase with temperature is observed in the luminescence intensity, yielding low activation energy, 3.8meV, which may be related to the Er excess at boundary layer.

In samples codoped with ytterbium, energy transfer process from  $\text{Yb}^{3+}$  to  $\text{Er}^{3+}$  has shown effective for  $\text{Er}^{3+}$  ions adsorbed at boundary layer. It has been observed emission about 1540nm either for samples excited indirectly, through pumping of  $\text{Yb}^{3+}$  ions and by excitation band-to band of  $\text{SnO}_2$  matrix as well as direct excitation of  $\text{Er}^{3+}$ . These results are in good agreement with previous data reported for 0.1at% Er  $\text{SnO}_2$  samples, where the rare-earth dopant enters substitutional to  $\text{Sn}^{4+}$  or remains segregated at particles surface.

#### Acknowledgement

The authors wish to thank Prof. José B. B. Oliveira and Prof. Américo S. Tabata for the use and help with the technical set-up, and CAPES, FAPESP, CNPq for financial resources.

- 
- [1] S. Coffa, G. Franzo, F. Priolo, A. Polman, and R. Serna, *Phys. Rev. B* **49**, 16313 (1994).
- [2] S. Komuro, T. Katsumata, T. Morikawa, X. Zhao, H. Isshiki, and Y. Aoyagi, *J. Appl. Phys.* **88**, 7129 (2000).
- [3] M. Ishii, S. Komuro, and T. Morikawa, *J. Appl. Phys.* **94**, 3823 (2003).
- [4] C. Li, K. Kondo, T. Makimura, and K. Murakami, *Appl. Surf. Sci.* **197-198**, 607 (2002).
- [5] E. Dien, J. M. Laurent, and A. Smith, *J. of the European Cer. Soc.* **19**, 787 (1999).
- [6] A. C. Yanes, J. Del Castillo, M. Torres, J. Peraza, V. D. Rodriguez, and J. Mendes-Ramos, *Appl. Phys. Lett.* **85**, 2343 (2004).
- [7] J. Rockenbecher, U. zum Felde, M. Tischer, L. Troger, M. Haase, and H. Weller *J. Chem. Phys.* **112**, 4296 (2000).
- [8] R. R. Goncalves, M. Ferrari, A. Chiasera, M. Montagna, E. A. Morais, L. V. A. Scalvi, C. V. Santilli, Y. Messaddeq, and S. J. L. Ribeiro, *J. Metastable Nanocryst. Mater.* **14**, 107 (2002).
- [9] H. Elhouichet, L. Othman, A. Moadhen, M. Oueslati, and J. A. Roger, *Mater. Sci. Eng. B* **105**, 8 (2003).
- [10] R. R. Gonçaves, G. Carturan, M. Montagna, M. Ferrari, L. Zampedri, S. Pelli, G. C. Righini, S. J. L. Ribeiro, and Y. Messaddeq, *Opt. Mater.* **25**, 131 (2004).
- [11] L. H. Slooff, M. J. A. De Dood, A. Van Blaaderen, and A. Polman, *J. Non-Cryst. Solids* **296**, 158 (2001).
- [12] E. A. Morais, S. J. L. Ribeiro, L. V. A. Scalvi, C. V. Santilli, L. O. Ruggiero, S. H. Pulcinelli, and Y. Messaddeq, *J. Alloys Compd.* **344**, 217 (2002).
- [13] T. Matsuoka, Y. Kasahara, M. Tsuchiya, T. Nitta, and S. Hagiwara *J. Electrochem. Soc.* **125**, 102 (1978).
- [14] T.D. Culp, J. G. Cederberg, B. Bieg, T.F. Kuech, K.L. Bray, D. Pfeiffer, and H.C. Winter, *J. Appl. Phys.* **83**, 4918 (1998).
- [15] W. X. Ni, K. B. Joelsson, C. X. Du, G. Pozina, L. A. Buyanova, W. M. Chena, G. V. Hansson, and B. Monemar, *Thin Solid Films* **321**, 223 (1998).